

# Zirconia-Based Sintered Ceramics for Osteoimplantology



Ales Buyakov<sup>1,2</sup>, Denis Kulbakin<sup>3</sup>, Svetlana Buyakova<sup>1,2</sup> and Sergey Kulkov<sup>1,2\*</sup>

<sup>1</sup>Department of Materials Science, Institute of Strength Physics and Materials Science, Russia

<sup>2</sup>Department of Microbiology, National Research Tomsk State University, Russia

<sup>3</sup>Department of Microbiology, Tomsk Cancer Research Institute, Russia

**Submission:** November 26, 2018; **Published:** March 28, 2019

**\*Corresponding author:** Sergey Kulkov, Department of Materials Science, Institute of Strength Physics and Materials Science, National Research Tomsk State University, Tomsk, 634050, Russia

## Abstract

It has been studied a porous ceramic obtained from ultra-fine powders. The porosity of ceramic samples sintered at different temperatures was up to 80 % and porous has a cellular structure. It has been shown that the most intensive densification of zirconia-based ceramics sintered from plasma-sprayed powders is took place during heating stage. It has been shown that during sintering of porous ceramic were formed bimodal porosity with mean size 25-30 and 90-110  $\mu\text{m}$ . Ceramic strength directly depends on micro stresses and at high micro stresses ceramic has a low strength. The main mechanical characteristics of the material were determined, and it was shown, that they are very close to the characteristics of natural bone tissues. It has been shown that this structure has positive effect on the pre-osteoblast cells proliferation. In-vitro studies of pre-osteoblast cells, cultivation on porous ceramic surface has shown a good cell adhesion, proliferation and differentiation of MMSC by osteogenic type.

**Keywords:** ceramic samples; zirconia; bimodal porosity; DNA processes; stabilization; magnesium oxide; Coherently Diffracted; parabolic factor

**Abbreviations:** UHMWP: Ultra-High Molecular Weight Polyethylene; CDD: Coherently Diffracted Domains; MMSC: Multipotent Mesenchymal Stem Cells; FBS: Fetal Bovine Serum;

## Introduction

Plasma spray synthesis and chemical co-precipitation methods are the main efficient routs for ultra-fine powder production as it's activated a sintering process [1]. The sintering process for these powders with identical chemical composition may be very different and final structure of a sintered body depends on a particle size, surface energy strain conserved in the whole system etc. [2]. For example, one can obtained hollow-ball particles, which forms will stipulate a special morphology structure of materials [3]. Applications of ceramics for using as bone-replacement material had a special interest now. The most actively developed studies in this area are investigations of zirconia ceramic ( $\text{ZrO}_2$ ) included in ISO register as a material for bone replacement. Ceramics based on zirconia stabilized with magnesium oxide ( $\text{MgO}$ ) besides with absence of chemically interaction with body tissues and resistant to most ways of sterilization, like  $\gamma$ -irradiation or steam autoclave treatment is advantage in comparison with other materials. Moreover, magnesium is involved in protein synthesis and DNA processes, stabilization of DNA molecules, RNA and ribosomes [4].

Nevertheless, as a material for replacement, zirconia-based ceramics has some disadvantages, such as high elasticity, low limiting

strain and low resistance to crack propagation in comparison with bone tissue. Solving the problem of biomechanical compatibility of zirconia-based implants may be creation of different type ceramic composites [3,5]. However, in literature there are small data about this system with a porosity close as comparable to inorganic bone matrix structure. The aim of the work is the investigation of densification, structure and mechanical properties of materials based on zirconia sintered at different temperatures and to study its biological properties for possibility for using in osteoimplantology.

## Materials and Experimental Procedure

Ceramic samples made from plasma-sprayed  $\text{ZrO}_2(\text{Y}_2\text{O}_3)$  and  $\text{ZrO}_2(\text{MgO})$  powders produced by Siberian Enterprise Chemical Group, following chemical process, as previously described [4], were studied. Samples were obtained by uniaxial compaction at 180 MPa followed by sintering at 1600  $^\circ\text{C}$  with isothermal exposure for one hour. For obtaining porosity approximately 45% to the mixtures add 50 vol.% of Ultra-High Molecular Weight Polyethylene (UHMWPE) particles with mean size 100  $\mu\text{m}$  which were removed during first sintering stage at 300  $^\circ\text{C}$  for one hour. In

the result were obtained porosity 43 - 49%. Structure investigation were carried out on the samples sintered in the temperature range 1400 - 1650 °C during isothermal holding from 1 up to 5 hours after uniaxial compression with the loading speed  $4 \times 10^{-4} \text{ s}^{-1}$ .

For determination of the exponent of the equation Hollomon ( $\sigma = K \varepsilon^k$ , when  $\sigma$  - true stress;  $\varepsilon$ - true strain; k - parabolic factor; K - constant) [5] all experimental data were re-plotted in "log-log" coordinates. For carrying out a phase identification and determination of the Coherently Diffracted Domains (CDD) [6,7], an X-ray analysis of ceramic materials was carried out using diffractometer with  $\text{CuK}\alpha$  radiation in angle interval  $10^\circ$ - $115^\circ$ , with step  $0.05^\circ$  and time exposure enough for statistical accuracy better 3%. The structure of the ceramics was studied by using scanning electron microscope Tescan Vega 3, mechanical properties were studied on test machine Devotrans GP.

To evaluate the biocompatibility of porous ceramic materials were used Multipotent Mesenchymal Stem Cells (MMSC) which had a typical fibroblastoid morphology, demonstrated the ability differentiate in adipogenic and osteogenic directions and satisfied the minimum criteria for multipotent mesenchymal stromal cells. MMSC were extracted from biopsies of subcutaneous fatty tissue by enzymatic method. Obtained cells were cultured in growth medium composition DMEM: F12, 10% Fetal Bovine Serum (FBS), 1 ng / ml basic fibroblast growth factor (b-FGF), 2 mM L-glutamine (Sigma-Aldrich, USA), 100 Uits / ml penicillin and 100 ug / ml

streptomycin (PAA, Austria) and multigas incubation C210 (Binder, Germany) at 37 °C, 5%  $\text{O}_2$  and 5%  $\text{CO}_2$ . Medium was changed every 3 days. To evaluate the cytotoxicity of porous ceramics samples and to determine the viability of cultured on ceramic surface cells were used a combined staining of cells with fluorescein diacetate (FDA; "Life Technologies", USA) and propidium iodide (PI; "Sigma", USA) after 24 hours and 7 days after inoculation.

To determine the ability MMSC to directed osteogenic differentiation during their cultivating on the surface of porous ceramic materials were performed detection of alkaline phosphatase as a first marker of osteogenic differentiation. For this purpose, were used a colorimetric method based on substrate BCIP / NBT: MMSC were seeded on the surface of ceramic samples and cultured for 14 days, then cells were fixed for 10 minutes in 4% paraformaldehyde, 0.5 ml of BCIP / NBT, and incubated at room temperature for 20 minutes, with following microscopy [8,9].

### Results and Discussion

Zirconia powder was characterized by spherical particles and their agglomerates, Figure 1 (a). An average particle size was 1.5  $\mu\text{m}$ . It was measured that specific surface of chemically precipitated powder was equal to 7  $\text{m}^2/\text{g}$ . According to the X-ray data the tetragonal phases of  $\text{ZrO}_2$  was predominant in the amount of 95 % with an average CDD size 20 nm. An average CDD size of monoclinic phase was equal to 20 nm and the same value we have obtained from size distribution in TEM investigations, Figure 1(b). This means that grains are mono-domain crystals.

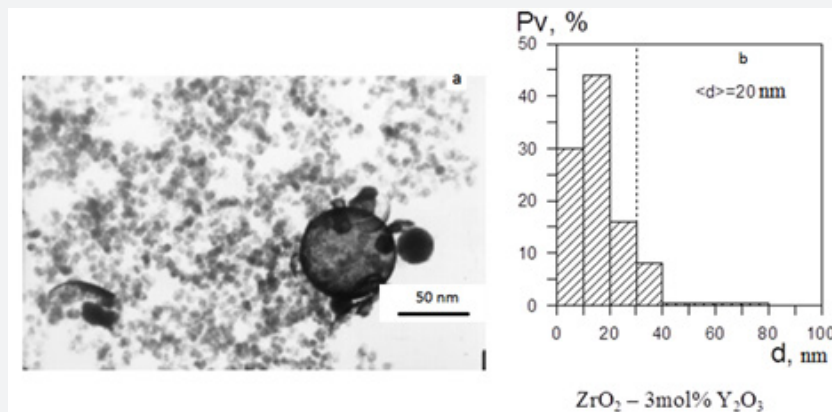


**Figure 1:** (a) TEM image of ZrO<sub>2</sub> powder, synthesized by plasma-sprayed method (b) and grain-size distribution.

Density dependences during sintering process are represented on Figure 2 and one can concludes that most intensive densification occurred at heating stage. The analyzing of this dependence using equation of the form  $\frac{\Delta L}{L} = K \tau^n$ ,  $\frac{\Delta L}{L}$  - relative shrinkage, K - kinetic coefficient; n - constant of densification rate, in log-log coordinates, were revealed that n for the samples made from plasma-sprayed powder is twice as much as for samples based on chemically precipitated powder; 0.1 and 0.04 accordingly [3]. X-ray analysis had shown, that the tetragonal phase content in sintered ceramics was decreasing with increasing of the holding time

up to 5 hours for materials based on plasma-sprayed powder from 95 up to 60 %, further increasing of holding time didn't influence the phase composition.

Stress-strain diagram of porous ceramics which were gained from plasma-sprayed method are presented on Figure 3. The obtained stress-strain diagrams had descending branch with a monotonic decrease of stress. It is an evidence of damages accumulation in the samples in contrast to the stress-strain diagrams of brittle materials with a homogeneous structure. On Figure 3(a) are shown the polished surface of the material and (b) pore size

distribution. As one can see, were formed porosity two types: with a mean size of 94  $\mu\text{m}$ , formed due to UHMWPE particles and with a mean size 27  $\mu\text{m}$ . Depending on the composition the average

pore size varied slightly in the range of 4 microns. Obviously, large pores are communicated with each other and may contribute MMSC cell adhesion at *in vitro* studies.

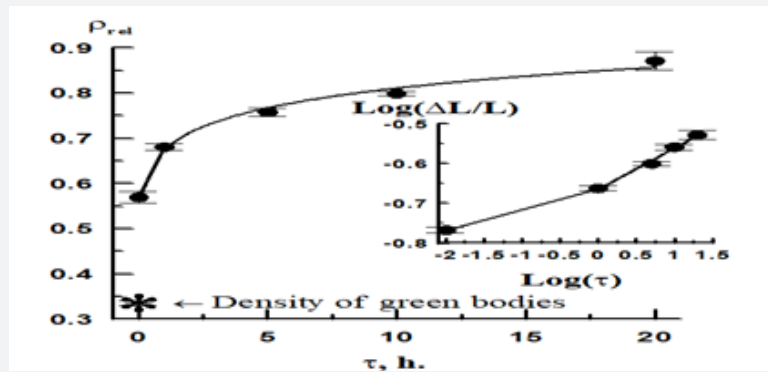


**Figure 2:** Dependences of relative density on the duration of isothermal holding for  $\text{ZrO}_2$  powder and kinetic dependences of samples shrinkage during isothermal holding.

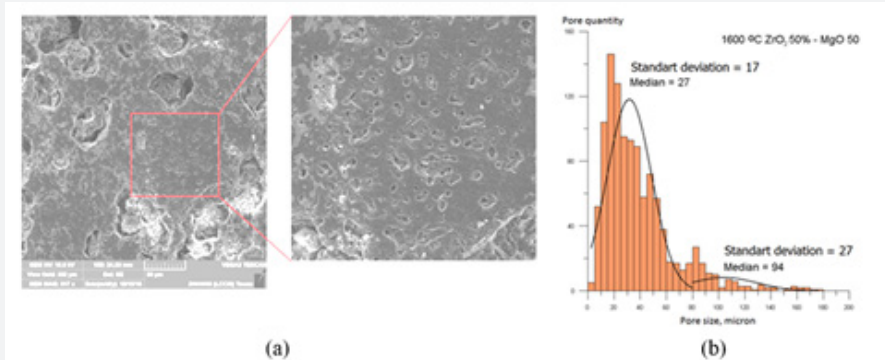


**Figure 3:** (a) - Surface of ceramic and (b) - pore size distribution in  $\text{ZrO}_2(\text{MgO})$  50% - MgO 50% ceramic.

**Table 1:** Properties of sintered composites.

MgO content, %	$\sigma$ , MPa	E, GPa	Mean pore size of small type, $\mu\text{m}$ and standard deviation	Mean pore size of second type, $\mu\text{m}$ and standard deviation
0	18.2	1.6	29; sd=19	110; sd=31
25	21	1.8	30; sd=23	104; sd=21
50	28.5	2.4	27; sd=17	94; sd=27
75	32.5	2.3	26; sd=17	101; sd=30
100	33.1	3	28; sd=20	105; sd=27

In a Table 1 are shown results of mechanical properties and mean pore size with different content of magnesia. As one can see, the maximal strength corresponds to MgO, 33 MPa and with increasing of  $\text{ZrO}_2(\text{Mg})$  content tensile strength reduce to 18 MPa. Figure 4(a) shows integral intensity of phases vs. MgO concentration. The intensity of  $\text{ZrO}_2$  cubic phase peaks decreases with increasing of magnesia concentration, but this dependence is non-linear, which can be explained by the different absorption coefficient of components. From X-ray patterns it have been calculated sizes of Coherent Diffraction Domains (CDD) of phases and its lattice micro distortions. It have been found that with increasing of MgO concentration the mean size of  $\text{ZrO}_2$  cubic phase crystallites

increases from 400  $\text{\AA}$  to 600  $\text{\AA}$ , while the micro distortions decrease from 0.025 to 0.01. MgO crystallites size almost does not change and its values approximately 60 nm, but lattice micro distortions decreases from 0.009 to 0.003. On the fracture surface mean size of CDD of zirconia and magnesia much larger, this may be stipulated intercrystallite type fracture [4, 5].

On Figure 4(b) were shown the micro stresses calculated from micro distortions vs. macro stresses obtained from mechanical tests. As one can see ceramics strength directly depends on micro stresses, this means that grain boundaries are very important in mechanical properties formation. Micro-damages appearing in

the material had local nature and the sample under load retained the ability to resist increasing load. A distinctive feature of all the  $\sigma - \varepsilon$  diagrams obtained in the experiment was their nonlinearity at low deformations which was described by the parabolic

law, Figure 5. Moreover, a cyclic loading of samples on parabolic section of diagrams did not reveal residual strain. Therefore, the nonlinearity in the stress-strain diagrams was due to the elastic deformation of ceramics with cellular structure.

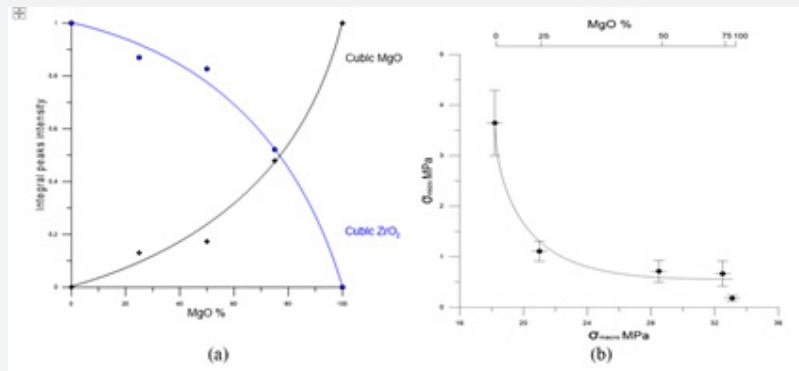


**Figure 4:** (a) Intensity of zirconia cubic phase and MgO of crystal lattice in the composition. (b) Dependence of micro- from macro stress of studied ceramics.

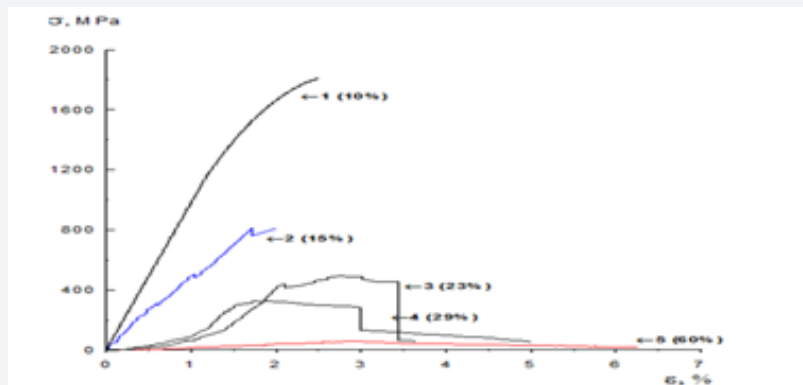


**Figure 5:** Stress-strain diagrams of sintered zirconia with different porosity

The structure of the ceramic materials produced from plasma-sprayed ZrO<sub>2</sub> powder was represented as a system of cell and rod structure elements, Figure 6. Cellular structure formed by stacking hollow powder particles can be easily seen at the images of fracture surfaces of obtained ceramics. There were three types of pores in ceramics: large cellular hollow spaces, small interparticle pores which are not filled with powder particles and the small-

est pores in the shells of cells. The cells generally did not have regular shapes. The size of the interior of the cells many times exceeded the thickness of the walls which was a single-layer packing of ZrO<sub>2</sub> grains. The increase of the pore space in the ceramics was accompanied by the decrease of the average size of voids inside the cells and the average grain size.

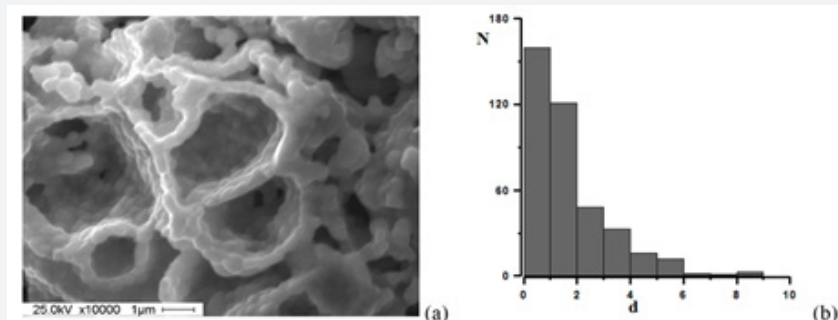


**Figure 6:** (a) Fracture surface of sintered ceramic samples (b) and pore size distribution for ZrO<sub>2</sub> with 40% porosity.

Re-plotting stress-strain diagrams in “log-log” coordinates allowed us to determine the exponent of the equation Holloman [5],  $k$  - parabolic factor from the experimental data. In this case, the index takes the value of the power function of the slope of the strain diagram in logarithmic scale. Analysis of stress-strain diagrams for ceramics with different porosity reveals that the expansion of the pore space volume in ceramics structure induces multiple microdamage during deformation; in so doing, the higher the porosity, the more pronounced the microdamage. This process is manifested in the diagrams as sharp stress drops due to microcracking. Microcracks are stops by pores and the material restores the possibility for an elastic deformation. The region of microcracking appearing with increasing of porosity is shifted to the area of high stresses and becomes more extended. The stress-strain diagrams for ceramics with porosity higher than 20 % are non-linear, which is absolutely atypical for the loading curves of sintered materials. The slopes in the curves  $\sigma = f(\varepsilon)$  under active loading up to microcracking change depending on the porosity value. Such dependences can be described by a power function of the type both for the process related with deformation and for the process related

with compaction of a porous solid, whose manifestation can be expected in the given system. In this case, the value of the exponent  $k$  is defined by which of the processes - compaction or plastic deformation is the governing one in this material. For purely elastic deformation  $k = 1$ , for plastic deformation  $k < 1$ , and for compaction  $k > 1$ .

Analysis of the dependence  $\sigma = f(\varepsilon)$  in logarithmic coordinates shows that diagrams for ceramics with porosity higher than ~ 20 % transform to several rectilinear portions and correspondingly have several values of  $k$ . The higher the porosity, the larger the number of linear portions that can be distinguished. The experimental values of  $k$  fit well into the three lines (Figure 7), i.e. there is a critical porosity value at which the deformation pattern of the porous solid changes drastically - a second exponent of the power function arises which is much higher than in the initial state. This is most likely associated with a change in the pore distribution pattern - from isolated pores to continuous porous structure. The material is actually divided into two subsystems deformed in different ways under external loading.

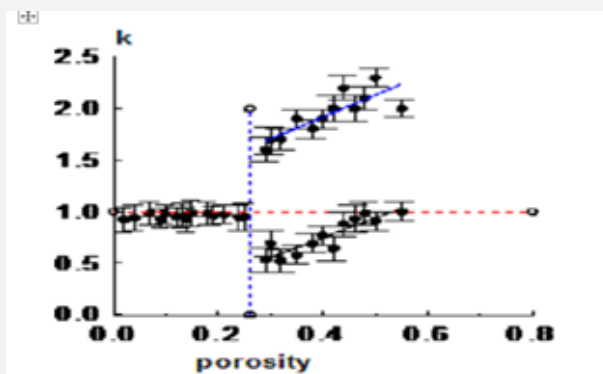


Figure 7: Parabolic factor of the deformation equation vs. porous space volume of sintered ZrO<sub>2</sub>.

No displacement of material volumes to the pore space has been found experimentally and we may thus assume that no compaction but only elastic deformation, i.e. elastic interaction of elementary volumes in the porous structure, takes place. These data were explained early [3,10,11], and it have been shown that in such system one can observed of losses deformation stability

of cell-like or rod-like structures formed in ceramics during sintering. According to these estimates, even at stability loss in rod-shaped structures with a small number of elements they may undergo noticeable macro deformation in the elastic region as structural elements, which are observed experimentally.

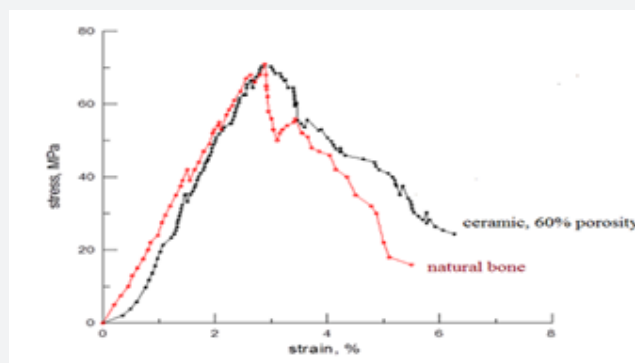
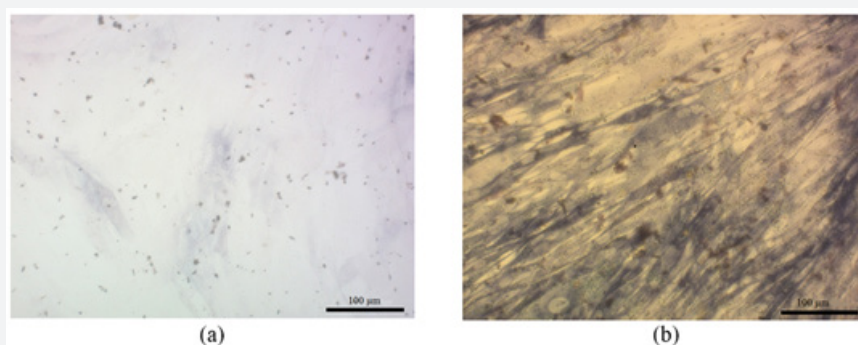


Figure 8: Parabolic factor of the deformation equation vs. porous space volume of sintered ZrO<sub>2</sub>.

Sintered ceramic with a high porosity obtained in this study has a very similar behavior as compare with natural bone, Figure 8. As one can see from figure a stress-strain diagrams of these materials has same peculiarities - microcracking on active loading and damages accumulation after maximum stresses. Therefore, this ceramic can be used as perspective material for bone replacement. Determining of MMSC ability to aimed osteogenic differentiation during their cultivating on the porous ceramic samples was performed by alkaline phosphatase detection, which is a first marker of osteogenic differentiation. Figure 9(a) shows undifferentiated MMSC which do not express or weakly express

alkaline phosphatase and give only background staining with adding of reagents. After 7 days of culturing were observed various degree of cells propagation with the highest activity on the composition with 25% of MgO concentration. Figure 9(b) shows the results after 14 days of cultivation in osteoinductive medium cells differentiate into osteogenic direction and give saturated media staining with colorimetric detection of alkaline phosphatase. The mean cell viability on the ceramic surfaces was about 93%, which is comparable to cell viability before planting. In addition, should be noted the presence of cell clusters in the pores, which may be described by their proliferation.



**Figure 9:** Detection of MMSC alkaline phosphatase. Transmitted light microscopy.

- a. Undifferentiated MMSC.
- b. Cultured for 14 days MMSC which differentiate into osteogenic direction are painted.

### Conclusion

- a. It has been shown that the most intensive densification of zirconia-based ceramics sintered from plasma-sprayed powders is took place during heating stage. It has been shown that during sintering of porous ceramic were formed bimodal porosity structure with mean size 25-30 and 90-110 µm.
- b. Ceramic strength directly depends on micro stresses and at high micro stresses ceramic has a low strength.
- c. It was shown that the “stress - strain” diagrams on the initial stage of deformation has a nonlinear behavior with high parabolic factor of strain-stress curves. It has been shown that fracture of the materials was observed from the elastic area and has rod-like or cellular-like parts in its structure.
- d. Sintered ceramic with a high porosity has a very similar behavior as compare with natural bone and can be used as perspective material for bone replacement.
- e. *In vitro* studies were showed that the tested materials are not cytotoxic, cultured MMS cells on the surface of the samples have high viability and osteogenic differentiation ability, and the presence of cell clusters in the pores of the samples may indicate their proliferation.

### Acknowledgment

This work was carried out according to the Program III.23 of Fundamental Scientific Research of the State Russian Academy of

Sciences for 2013-2020 and Program of Tomsk State University competitiveness improvement program, Project #8.2.14.2018.

### References

1. Fedorchenko IM, Ivanova II (1974) About influence of particle size and specific surface on densification during the sintering Theory and technology of sintering, Kiev: Naukova Dumka, pp. 193-199.
2. (2001) Gusev AI, Rempel AI (2001) Nanocrystalline materials Moscow: Physmathlit, 224.
3. Kulkov SN, Buyakova SP (2007) Structure, phase composition and technologies features of zirconia-based nano systems Russian nanotechnology 2 (1): 119 -132.
4. E.Kalatur, S Buyakova S Kulkov, A Narikovich (2014) Porosity and Mechanical Properties of Zirconium Ceramics. AIP Proceedings, Melville, New York, 1623, pp. 225-228.
5. Hertzberg RW (1989) Deformation and fracture mechanics of engineering materials John Wiley and Sons, Inc pp. 576.
6. (1984) Torayda H, Yoshimura M, Somiya S J Am Ceram Soc 6(6): 119-121
7. Gorelic SS, Skakov YuA, Rastorguev (1994) LN X-ray and electron optical microscope analysis M: MISIS, pp. 327.
8. Gutsol AA, Sokhnevich NA, Yurova KA, Khaziakhmatova OG, Shupletsova VV (2015) Dose-dependent effects of dexamethasone on functional activity of T-lymphocytes with different grades of differentiation Molecular Biology 49(1): 130-137.
9. Dominici M, Le Blanc K, Mueller I, Slaper-Cortenbach I, Marini F, et al. (2006) Minimal criteria for defining multipotent mesenchymal stromal cells, The International Society for Cellular Therapy position statement. Cryotherapy 8(4): 315-317.

10. Kolmakova T, Buyakova S, Kulkov S (2015) Research of mechanics of the compact bone microvolume and porous ceramics under uniaxial compression." In NEW OPERATIONAL TECHNOLOGIES (NEWOT'2015): Proceedings of the 5<sup>th</sup> International Scientific Conference New Operational Technologies. 1688. AIP Publishing.
11. Kulkov S, Buyakova S (2015) Porosity and mechanical properties of zirconium ceramics. New Operational Technologies (Newot 2015): Proceedings of the 5th International Scientific Conference New Operational Technologies. 1688 AIP Publishing.



This work is licensed under Creative Commons Attribution 4.0 License  
DOI: [10.19080/AIBM.2019.13.555867](https://doi.org/10.19080/AIBM.2019.13.555867)

**Your next submission with Juniper Publishers  
will reach you the below assets**

- Quality Editorial service
- Swift Peer Review
- Reprints availability
- E-prints Service
- Manuscript Podcast for convenient understanding
- Global attainment for your research
- Manuscript accessibility in different formats  
**( Pdf, E-pub, Full Text, Audio )**
- Unceasing customer service

**Track the below URL for one-step submission**  
<https://juniperpublishers.com/online-submission.php>